The Journal of Chemical Physics ARTICLE scitation.org/journal/jcp

Time-scale ordering in hydrogen- and van der Waals-bonded liquids

Cite as: J. Chem. Phys. 154, 184508 (2021); doi: 10.1063/5.0049108
Submitted: 1 March 2021 • Accepted: 22 April 2021 •
Published Online: 14 May 2021

Lisa Anita Roed, Jeppe C. Dyre, Kristine Niss, Tina Hecksher, and Birte Riechers[a]

AFFILIATIONS

Glass and Time, IMFUFA, Department of Science and Environment, Roskilde University, P.O. Box 260, DK-4000 Roskilde, Denmark

[a]**Current address:** Federal Institute of Materials Research and Testing (BAM), Unter den Eichen 87, 12205 Berlin, Germany.
Author to whom correspondence should be addressed: birte.riechers@bam.de

ABSTRACT

The time scales of structural relaxation are investigated on the basis of five different response functions for 1,2, 6-hexanetriol, a hydrogen-bonded liquid with a minor secondary contribution, and 2,6,10,15,19,23-hexamethyl-tetracosane (squalane), a van der Waals-bonded liquid with a prominent secondary relaxation process. Time scales of structural relaxation are derived as inverse peak frequencies for each investigated response function. For 1,2,6-hexanetriol, the ratios of the time scales are temperature-independent, while a decoupling of time scales is observed for squalane in accordance with the literature. An alternative evaluation approach is made on the squalane data, extracting time scales from the terminal relaxation mode instead of the peak position, and in this case, temperature-independent time-scale ratios are also found for squalane, despite its strong secondary relaxation contribution. Interestingly, the very same ordering of response-function-specific time scales is observed for these two liquids, which is also consistent with the observation made for simple van der Waals-bonded liquids reported previously [Jakobsen *et al.*, J. Chem. Phys. **136**, 081102 (2012)]. This time-scale ordering is based on the following response functions, from fast to slow dynamics: shear modulus, bulk modulus, dielectric permittivity, longitudinal thermal expansivity coefficient, and longitudinal specific heat. These findings indicate a general relation between the time scales of different response functions and, as inter-molecular interactions apparently play a subordinate role, suggest a rather generic nature of the process of structural relaxation.

I. INTRODUCTION

The dynamics of structural relaxation in amorphous matter show tremendous temperature-imposed changes, resulting in structural response time scales, τ, spanning up to 15 orders of magnitude.[1–3] In the liquid regime, structural relaxation times are in the picosecond range, whereas deeply supercooled liquids, for which the equilibrium state can barely be reached, have response time scales of $\tau \approx 1000$ s.

From an experimental point of view, the time scale of structural response can be assessed in multiple ways, e.g., by dielectric and mechanical spectroscopy, but also based on light-scattering,[4] calorimetric,[5] or aging measurements.[6] Time scales can be determined from the loss-peak position in spectral data, from auto-correlation functions based on time-domain data, or from the so-called *terminal* mode, which reflects the slowest spectral response such as the Maxwell relaxation time, τ_M.[7] Interestingly, time scales obtained from different response functions are not identical, even if determined the same way, e.g., via the spectral loss-peak position. The relation of time scales for two different response functions X_1 and X_2 is conveniently quantified by the following *time-scale index*: $\log \tau_{X_1}(T) - \log \tau_{X_2}(T)$.

If both sets of time scales have the same dependence on temperature, T, the time-scale index becomes temperature-independent. This *coupling* of time scales is observed for various pairs of response functions for a range of molecular glass formers.[8] Several experimental studies report this behavior on the basis of data for the dielectric permittivity, ε, and the dc conductivity, σ, for phenyl salicylate, propylene carbonate, phenolphthaleine-dimethyl-ether, and various mono-alcohols,[9] the viscosity, η, for e.g., *o*-terphenyl, squalane, and glycerol,[10–12] calorimetric data on 5-polyphenyl-4-ether (5PPE),[5] and the dynamic shear modulus, $G(\omega)$, for 5PPE, 1,3-butandiol, and other molecular liquids.[13–15] Constant time-scale indices have also been reported for shear- and

bulk-mechanical data on 5PPE, tetramethyl-tetraphenyl-trisiloxolane (DC704), 1,2,6-hexanetriol, and more.[16–18] Other studies report dynamic response data that exhibit not only temperature- but also pressure-independent time-scale indices.[19,20]

The observation of *decoupling* in a set of response-function-specific time scales, i.e., the observation of a temperature-dependent time-scale index, is often attributed to the influence from other relaxation contributions rather than from the dynamics of the structural-relaxation process itself.[15,21,22] In the case of hydrogen-bonded liquids, which exhibit stronger intermolecular interactions than van der Waals (vdW)-bonded liquids, the formation of supramolecular structures is presumably reflected by a slow relaxation process, which can also affect the overall peak position[23,24] and thus the coupling behavior.

While the aforementioned studies mainly reported on the coupling tendencies that were observed for different sets of response functions, Jakobsen *et al.*[8] put the focus on the ordering of the time-scale indices connected to the probed response functions. In their study, time scales were determined for seven different response functions for the two vdW-bonded glass formers, 5PPE and DC704. These two materials exhibit simple behavior in terms of a non-detectable secondary relaxation process and obedience to time–temperature superposition.[25] Time scales differ significantly between response functions while their temperature-dependence is the same, and obey a response-function-specific ordering that is identical for both investigated liquids,

$$\tau_G < \tau_K < \tau_\varepsilon < \tau_{\alpha_l} < \tau_{c_l}.$$

The time scales are based on measurements of the following response functions: the shear-mechanical modulus $G(\omega)$, the bulk-mechanical modulus $K(\omega)$, the dielectric permittivity $\varepsilon(\omega)$, the longitudinal thermal expansion coefficient $\alpha_l(t)$, and the longitudinal specific heat $c_l(\omega)$.[8]

To test how general the response-function-dependent ordering of time-scale indices is, more complex liquids have to be put under investigation. Two aspects that are relevant in this context are (1) the interference of additional relaxation processes with the primary relaxation process as it has an impact on time scales derived from spectral data and (2) the influence of inter-molecular interactions on the different response functions.

Thus, in this study, the dynamics of two non-simple liquids with significantly different properties regarding the bonding type and relaxation processes are analyzed for five different experimental response functions. These two liquids are 1,2,6-hexanetriol (hexanetriol), a hydrogen-bonded liquid with a weak secondary contribution, and 2,6,10,15,19,23-hexamethyltetracosane (squalane), a vdW-bonded liquid with a strong secondary relaxation. Time-scale coupling, i.e., the observation of a temperature-independent time-scale index, is reported for hexanetriol, while squalane shows decoupling of the time scales if these are determined from spectral loss-peak positions. If time scales are derived from terminal modes of spectra measured on squalane, response-specific time scales exhibit less decoupling and identical response-specific ordering of time-scale indices is observed for both vdW-bonded and hydrogen-bonded liquids.

In this article, Sec. II describes briefly the methods used for obtaining the five different response functions. In Sec. III, data that were measured on these response functions for hexanetriol and squalane are subdivided into three parts. Section III A contains spectral data, Sec. III B presents time scales of structural relaxation, and in Sec. III C, the time-scale indices obtained for hexanetriol and squalane are discussed and compared to results for the simple vdW-liquid DC704 as presented in Ref. 8.

II. EXPERIMENTAL METHODS

Temperature-dependent time-scale data were obtained for the following five response functions: the shear modulus $G(\omega)$, the bulk modulus $K(\omega)$, the dielectric permittivity $\varepsilon(\omega)$, the longitudinal thermal expansion $\alpha_l(t)$, and longitudinal specific heat $c_l(\omega)$. The transducers used for measuring these response functions are customized for usage within the same cryostat (available temperature range from 100 to 310 K), ensuring comparable thermal conditions involving a steady absolute temperature over weeks and restricting temperature fluctuations to few mK.[26] Response functions are determined with the same electronics system on the basis of electrical measurements.[27] Shear-mechanical measurements were conducted with the piezo-electric shear-modulus gauge that allows for measurements at frequencies $\nu = \omega/(2\pi)$ between 1 mHz and 50 kHz.[28] Bulk-modulus data were obtained with a piezo-electric bulk-modulus gauge (frequency range 1 mHz–10 kHz).[29] Dielectric permittivity data are based on measurements with a parallel-plate capacitor (fixed spacing of 50 μm) within the available frequency range (1 mHz–1 MHz). For squalane, the dielectric dataset was supplemented by measurements with an Andeen Hagerling 2700A high-resolution capacitance bridge (frequency range is 50 Hz to 20 kHz). Time-dependent thermal expansion data are based on high-resolution dielectric dilatometry measurements at a fixed frequency under fast temperature regulation using a parallel-plate capacitor in which the sample material controls the spacing.[30] Dynamic specific-heat data were measured using a negative temperature-coefficient thermistor simultaneously serving as a temperature gauge and heating device in the available frequency range from ~5 mHz to 20 Hz.[31,32] The quantity derived from these measurements is the longitudinal specific heat, $c_l(\omega)$, which corresponds to the heat needed to increase the temperature by one unit if the associated expansion is restricted to be longitudinal instead of isotropic.[33] Short reviews of the different measurement principles are given in the supplementary material.

Experimental data were acquired for the two different molecular glass formers, hexanetriol and squalane. Hexanetriol is a hydrogen-bonding trihydric alcohol ($T_g \cong 200$ K) with a secondary process occurring in the form of an excess wing[16,34] and similar properties to glycerol. The slightly higher glass transition temperature, however, makes hexanetriol a more suitable candidate for meeting the temperature limitation and the narrow frequency window of the specific-heat measurement technique.[34] The complex, frequency-dependent shear modulus $G(\omega)$, bulk modulus $K(\omega)$, dielectric permittivity $\varepsilon(\omega)$, and longitudinal specific heat $c_l(\omega)$ were measured for hexanetriol under identical experimental conditions, i.e., within the same cryostat and with the same electronic setup. As hexanetriol has a significant dipole moment, the determination of the thermal expansion coefficient based on dielectric dilatometry is not feasible.[30] Hexanetriol was purchased from Sigma-Aldrich with a purity of 96% and used as received.

The container was opened in a dry N_2 atmosphere to avoid contamination with water. The sample cells were prepared and filled in a dry N_2 atmosphere, with the exemption of the bulk-modulus measurements, for which the transducer was filled in ambient air.

Squalane is a vdW-bonded liquid ($T_g \cong 168$ K) with a strong secondary relaxation peak in both mechanical and dielectric data. The complex dynamic shear modulus $G(\omega)$, bulk modulus $K(\omega)$, and dielectric permittivity $\varepsilon(\omega)$ measured in one cryostat are complemented by data of the longitudinal thermal expansion coefficient $\alpha_l(t)$ that was obtained in another cryostat. The temperatures of the two cryostats were calibrated based on the peak positions of dielectric data, which were available for both cryostats, resulting in a shift of the expansivity data by 0.80 K. Note that the bulk-modulus dataset was published in Ref. 35, and the dynamic thermal-expansion data are from the experiment presented in Ref. 36.

III. RESULTS

A. Spectral data

In this section, the frequency-dependent response functions for hexanetriol and squalane are presented. These are the real and imaginary parts of the shear modulus $G(\omega)$, the bulk modulus $K(\omega)$, the dielectric permittivity $\varepsilon(\omega)$, and the longitudinal specific heat $c_l(\omega)$ in the case of hexanetriol. For squalane, the loss contributions of the shear modulus $G''(\omega)$, the bulk modulus $K''(\omega)$, and the dielectric permittivity $\varepsilon''(\omega)$, are presented.

1. Hexanetriol

The storage and loss contributions of the dynamic shear modulus are plotted in Fig. 1 for selected temperatures between 200 and 220 K. At each temperature, two spectra were measured successively. As these data coincide within the accuracy of the measurement technique, full equilibration of the sample material at all depicted temperatures is assumed. Measurements of the dynamic bulk-mechanical modulus were conducted in the temperature range between 202 and 224 K measured in 1 K steps with a single spectrum measured at each temperature (Fig. 2).

Both the shear- and the bulk-modulus data show the characteristic features of a structural relaxation process. The storage contribution of the shear modulus approaches zero for frequencies $\nu \ll \nu_{lp}$, while the bulk modulus approaches the static contribution $K(0)$ in this limit. For both moduli, the loss contributions exhibit a power-law behavior with exponent 1 on the low-frequency flank. The spectra are rather broad, indicative of a slow relaxation process as previously reported for glycerol.[23,24] Based on the conclusions drawn for glycerol, the relaxation feature of hexanetriol may derive from supramolecular structure dynamics reflecting interactions between the various OH-groups of adjacent molecules. Additionally, at all temperatures, the signature of a secondary process is observed at high-frequencies, where both $G''(\omega)$ and $K''(\omega)$ exhibit a shoulder. This shoulder is more separated from the main process at low temperatures, but merges with the primary relaxation process at higher temperatures. This aspect is also evident in the high-frequency regime of the storage contribution, where the data steadily increase instead of reaching a constant plateau.

The dielectric permittivity was measured at 25 temperatures between 200 and 250 K. The loss and storage contributions are plotted in Fig. 3 for selected temperatures. At most temperatures, two subsequent spectra were measured and the collapse of these demonstrates a well-equilibrated state of the material. The dielectric loss spectra show the expected power law on the low-frequency flank

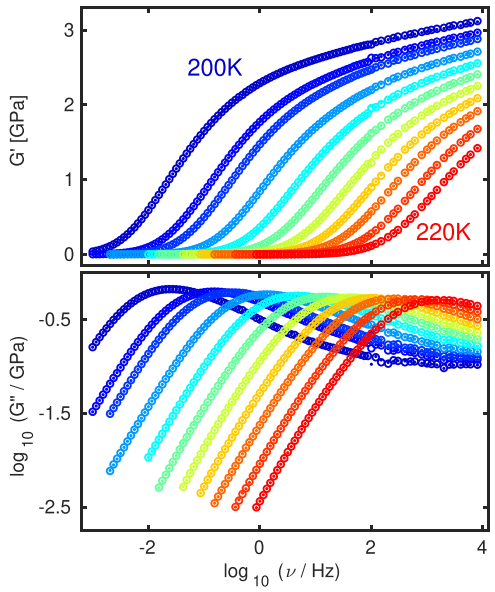

FIG. 1. Storage and loss spectra of the dynamic shear modulus $G(\omega) = G'(\omega) + iG''(\omega)$ of the supercooled liquid state of hexanetriol at selected temperatures ranging from 200 to 220 K. After quenching to 200 K, the shear modulus was measured in steps of 1 K from 202 to 214 K and steps of 2.5 K from 215 to 220 K. Points correspond to the first and open circles to the second, subsequently measured spectrum.

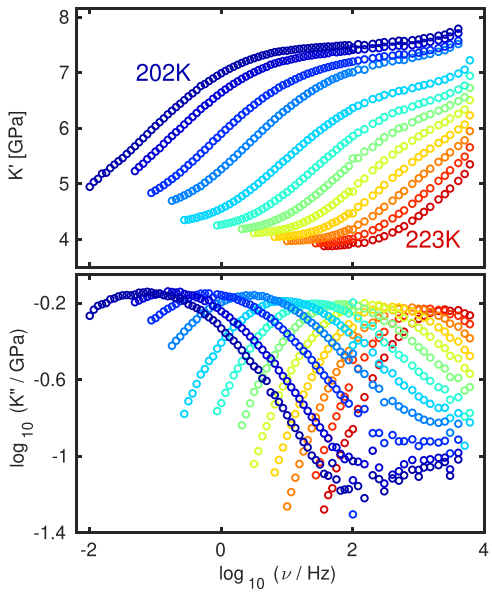

FIG. 2. Storage and loss spectra of the dynamic bulk modulus $K(\omega) = K'(\omega) + iK''(\omega)$ of the supercooled liquid state of hexanetriol for selected temperatures between 202 and 223 K. Spectra were measured from 223 to 203 K in steps of −2 K and from 202 to 222 K in steps of 2 K.

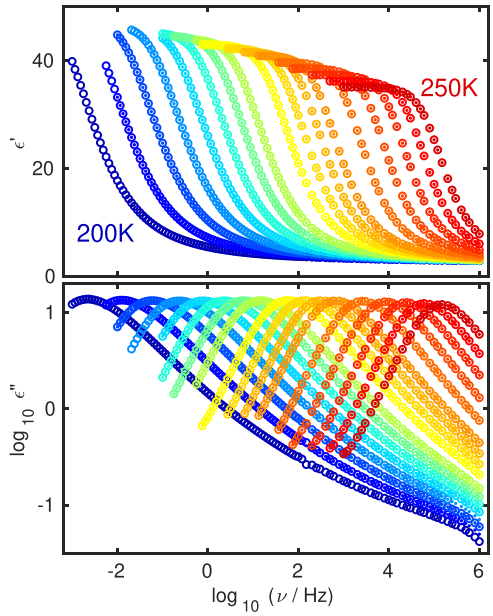

FIG. 3. Storage and loss spectra of the dynamic dielectric permittivity $\varepsilon(\omega) = \varepsilon'(\omega) - i\varepsilon''(\omega)$ of the supercooled liquid state of hexanetriol at selected temperatures ranging from 200 to 250 K. After a quench to 200 K, the spectra were measured in temperature steps of 1 K up to 215 K, steps of 2.5 K from 217.5 to 225 K, and steps of 5 K from 230 to 250 K. Points correspond to the first and open circles to the second, subsequently measured spectrum.

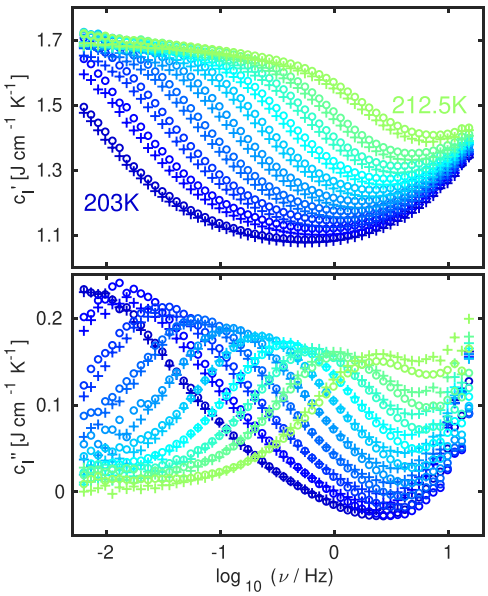

FIG. 4. Storage and loss spectra of the dynamic longitudinal heat capacity $c_l(\omega)$ in the supercooled liquid state of hexanetriol at temperatures ranging from 203 to 212.5 K. Crosses and circles reflect measurements at two different temperature amplitudes.

with an exponent of 1, as well as the power law behavior with an exponent of −1/2 on the high-frequency flank, indicating that the influence of the secondary relaxation contribution is negligible within the measured range of dielectric data. As is the case for glycerol, hexanetriol is expected to form a branched network of OH-bonds that gives no directional preference for an effective dipole moment,[23] reflected by the absence of a slow process on the low-frequency flank.

Figure 4 shows loss and storage contributions of the dynamic longitudinal heat capacity $c_l(\omega)$ at ten temperatures in the supercooled liquid, measured at two different temperature amplitudes. Both amplitudes yield a response within the linear regime and deviations between spectra at a given temperature indicate the uncertainty of the data. Two distinct artifacts are observed for $c_l(\omega)$, emphasizing that the accuracy of the details of the measured spectra of the longitudinal heat capacity is limited compared to the other measured response functions: first, the spectra measured at low temperatures exhibit slightly negative values of the imaginary part in the frequency range around 1 Hz. Second, both storage and loss contributions show increasing values at high frequencies. If the increase in c_l'' was solely due to a secondary contribution, c_l' would show a stepwise decrease toward a high-frequency plateau based on Kramers–Kronig relations. Despite these issues, normalizing the loss spectra to the amplitude and position of the maximum results in a reasonable collapse [see Fig. S2(d) in the supplementary material]. This emphasizes that the spectra obey time–temperature-superposition despite the limited accuracy in details of their shape. Thus, it seems reasonable to extract ν_{lp} for comparison to other time scales.

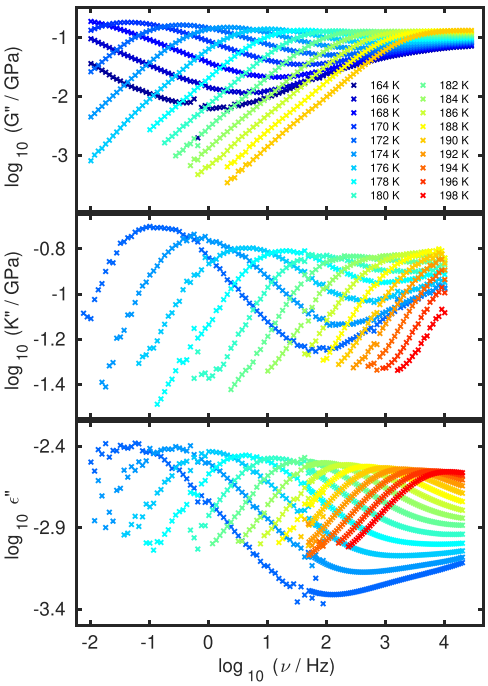

FIG. 5. Loss spectra of the dynamic shear modulus $G(\omega)$, bulk modulus $K(\omega)$, and dielectric permittivity $\varepsilon(\omega)$ of squalane from 164 to 190 K for shear-mechanical data, and from 172 to 198 K for dielectric and bulk-mechanical data.

2. Squalane

For a range of temperatures, Fig. 5 shows the loss contributions $\varepsilon''(\omega)$, $G''(\omega)$, and $K''(\omega)$ of squalane as functions of frequency. All three response functions show qualitatively comparable features: a primary relaxation contribution with a strongly temperature-dependent loss-peak position and a secondary contribution at higher frequencies with a comparably static loss-peak position, which merge upon increasing temperature.

However, details of the loss spectra of these three response functions differ significantly in their low-frequency behavior. The shear-mechanical data exhibit a power law behavior with an exponent close to unity (see Fig. S2 in the supplementary material), which thus resembles the rather universal behavior reflected by the response functions measured on hexanetriol. In the case of the bulk-mechanical and dielectric responses of squalane, however, the exponent of the low-frequency flank is significantly reduced to values around 0.3–0.4. This behavior might be a consequence of the rather small signal amplitudes of the two datasets, especially in the case of the dielectric data.

B. Time scales of structural relaxation

Loss spectra of the four response functions $G(\omega)$, $K(\omega)$, $\varepsilon(\omega)$, and $c_l(\omega)$ recorded at 210 K are plotted as functions of frequency for hexanetriol in Fig. 6(a). In this direct comparison, it can be seen that the specific heat and dielectric loss-peaks are narrower than those of the mechanical data. Both bulk- and shear-mechanical moduli show rather rounded features on the low-frequency flank, indicating the existence of an additional, slow relaxation process as reported for glycerol.[23,24]

The maximum-loss frequency $\nu_{lp,X}$ was identified as the loss-peak frequency for each frequency-dependent response function X. Assuming that the slow process proposed for hexanetriol has a negligible influence on the peak position, and as the spectra only show a minor secondary process, $\tau_X = (2\pi\nu_{lp,X})^{-1}$ reflects the time scale of structural relaxation. From $G(\omega)$, the Maxwell time scale τ_M was determined based on the relation $\tau_M = \eta_0/G_\infty$, in which the viscosity $\eta_0 = G''(\omega)/\omega|_{\omega\to 0}$ was deduced from the mechanical data and G_∞ was found from fits of the shear-mechanical data to an electrical-equivalent-circuit (EEC) model (see the supplementary material for details on the fitting function and parameters, as well as the temperature-dependence of G_∞). The temperature dependence of the five response-function-specific time scales for hexanetriol is depicted in Fig. 6(b). Note that the order of these time scales at a given temperature, as shown in Fig. 6(a), is maintained throughout the temperature range over which all response functions were measured (203–212.5 K), covering changes in τ of more than two orders of magnitude. The time scales determined from the two mechanical measurements are very similar, with shear-mechanical data showing slightly faster response behavior than the dynamic bulk-mechanical data. The dielectric and specific heat data exhibit a significantly slower relaxational response at a given temperature compared to the other response functions. Thus, hexanetriol exhibits the same ordering as simple vdW-bonded liquids.[8]

For squalane, the loss spectra of $G(\omega)$, $K(\omega)$, and $\varepsilon(\omega)$ measured at 178 K are plotted in Fig. 7(a). For all three response functions, a secondary relaxation contribution is seen as an onset of a second peak on the high-frequency part of the spectra. In contrast to the shear-mechanical response, the low-frequency flanks of bulk-mechanical and dielectric data are broadened. These features might be connected to the small dielectric response amplitudes for squalane and a presumably non-ideal match of bulk-mechanical data with its reference measurement, emphasizing that the data acquisition with these two methods is pushed to its limits due to

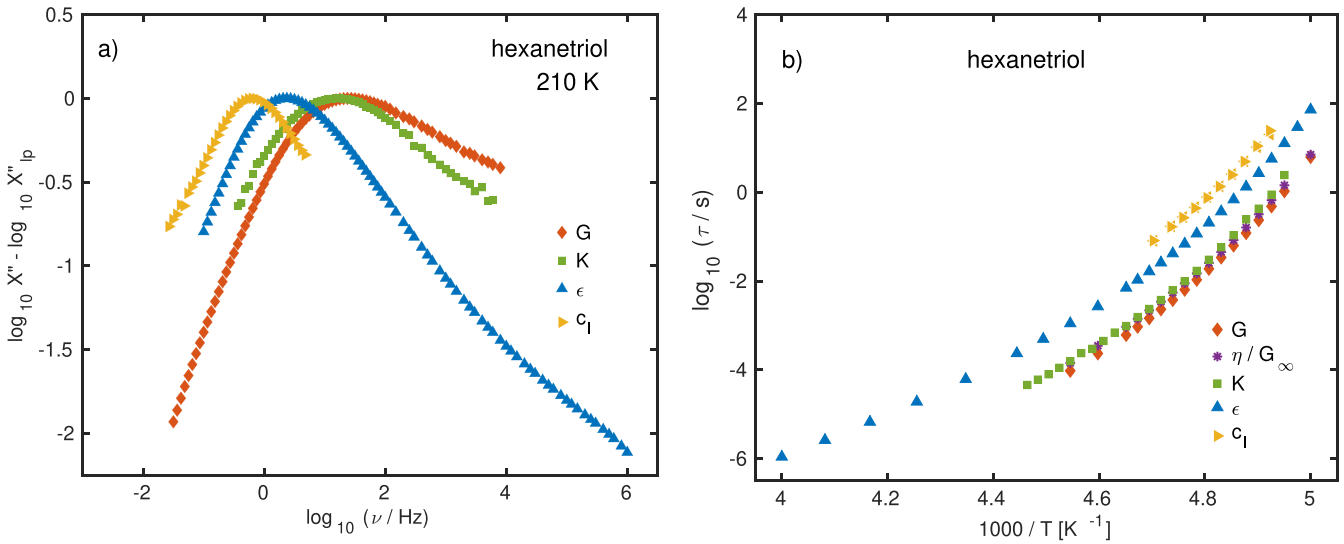

FIG. 6. (a) Loss contributions of four complex frequency-dependent response functions: the shear modulus $G(\omega)$, the bulk modulus $K(\omega)$, the dielectric permittivity $\varepsilon(\omega)$, and the longitudinal specific heat $c_l(\omega)$, as functions of frequency at 210 K for hexanetriol, normalized to the individual loss-peak height. (b) Time scales based on the spectral loss-peak positions of the four response functions depicted in (a) and Maxwell time scale as functions of the inverse temperature for hexanetriol. Specific heat data measured at two different temperature amplitudes are depicted as triangles pointing left and right.

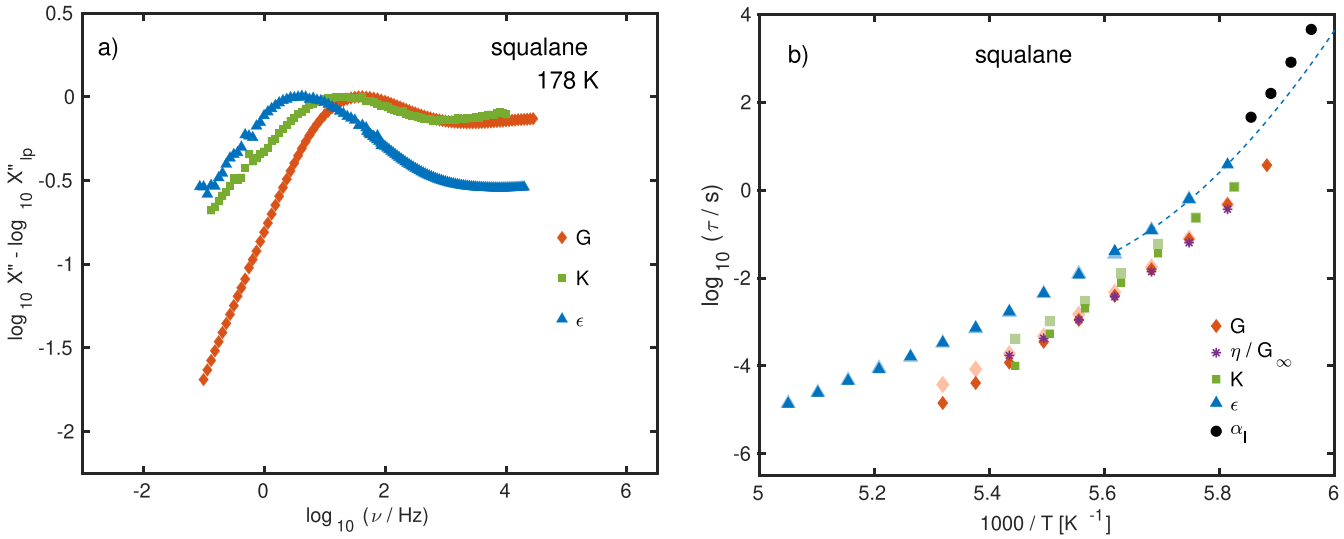

FIG. 7. (a) Loss contributions of three complex frequency-dependent response functions: the shear modulus $G(\omega)$, the bulk modulus $K(\omega)$, and the dielectric permittivity $\varepsilon(\omega)$, as functions of frequency at 178 K for squalane, normalized to the individual loss peak height. (b) Strong colors: time scales based on the spectral loss-peak positions of the three response functions depicted in (a) and time scales derived from expansivity data, plotted as functions of the inverse temperature for squalane. Light colors: time scales based on the spectral shift of the low-frequency flank relative to a low-temperature loss-peak-position derived time scale. The dashed line corresponds to a fit of the dielectric data between 172 and 180 K to a parabolic function with the parameters $\log_{10}\tau_0 = -2.13$, $J = 4051$ K, and $T_0 = 185.0$ K.

the low response amplitudes of squalane. The squalane time scales extracted from the spectral positions of the loss peaks are plotted against the temperature in Fig. 7(b). The time scales connected to the thermal expansion coefficient, τ_{α_l}, were determined from Laplace-transformed time-domain data measured by dielectric dilatometry (data are included in the supplementary material). As for hexanetriol, the mechanical data show smaller time scales than the dielectric measurements. The observed shift by one order of magnitude is in accordance with the data reported in Ref. 11. The expansivity data exhibit the largest time scales based on an extrapolation of the temperature dependence of dielectric data toward lower temperatures by a parabolic function $\tau(T) = \tau_0 \cdot \exp\left(J^2(1/T - 1/T_0)^2\right)$ [dashed line in Fig. 7(b)][8,37] as there is no overlap in temperature for dielectric and expansivity data.

When comparing τ_M and the loss-peak-derived τ_G, a deviation between the two is observed at high temperatures. A second approach was applied to extract the time scales of squalane, which focuses on the spectral position of the terminal mode. To do so, the spectra were manually shifted along the frequency-axis to collapse on the low-frequency flank. Relative to a loss-peak-derived time scale in the low-temperature regime of a dataset, the time scales were determined from the time–temperature-superposition related shift [light-colored symbols in Fig. 7(b)]. The error bars indicate the range of uncertainty for the shift factor and result from scatter of the spectral data in the low-frequency range. A visualization of the collapse of the spectral data based on the manual shift is included in the supplementary material.

C. Time-scale indices

To evaluate the temperature dependence of the time scales for the different response functions of hexanetriol and squalane, in the following, we define the time-scale index as the logarithm of the ratio of the dielectric time scale and the time scale of another response function X, $\log\tau_\varepsilon - \log\tau_X$. The normalization utilizes an interpolation of measured values of τ_ε within the temperature range of dielectric data for each material. At temperatures below this range, an extrapolation by a parabolic function based on the low-temperature dielectric data is applied.[8,37] Thus, in the case of squalane, time-scale indices for expansivity and low-temperature shear-mechanical data are based on extrapolated dielectric dynamics and will depend on the function used for extrapolation. A parabolic function was applied as it resulted in the most robust extrapolation of the experimental time-scale data in Ref. 8. Deriving τ_{α_l} from time-domain data and extrapolating the low-temperature dielectric time scale lead to a higher uncertainty of the time-scale index for expansivity data and thus do not allow for detailed conclusions on the coupling tendency.

In Fig. 8(a), the time-scale indices are plotted for hexanetriol. While τ_G is based on the spectral position of the loss peak maximum, τ_M reflects the position of the terminal mode at the low-frequency flank of the relaxation spectrum. Both time scales exhibit a temperature-independent time-scale index close to 1 for hexanetriol, suggesting only minor influence on the temperature dependence from the slow relaxation mode that is observed in the mechanical spectra.[23] τ_G and τ_K are approximately one order of magnitude smaller than τ_ε, which is half a magnitude smaller than the time-scale index of the heat capacity. The error on τ_{c_l} is determined based on the spectral positions of the loss-peak maximum before and after correction for method-specific temperature-independent features of the specific-heat data (see Ref. 32 for details). From this set of response functions, it becomes obvious that the specific time scales can differ by as much as 1.5 orders of magnitude at a given temperature. The general behavior of the time-scale indices

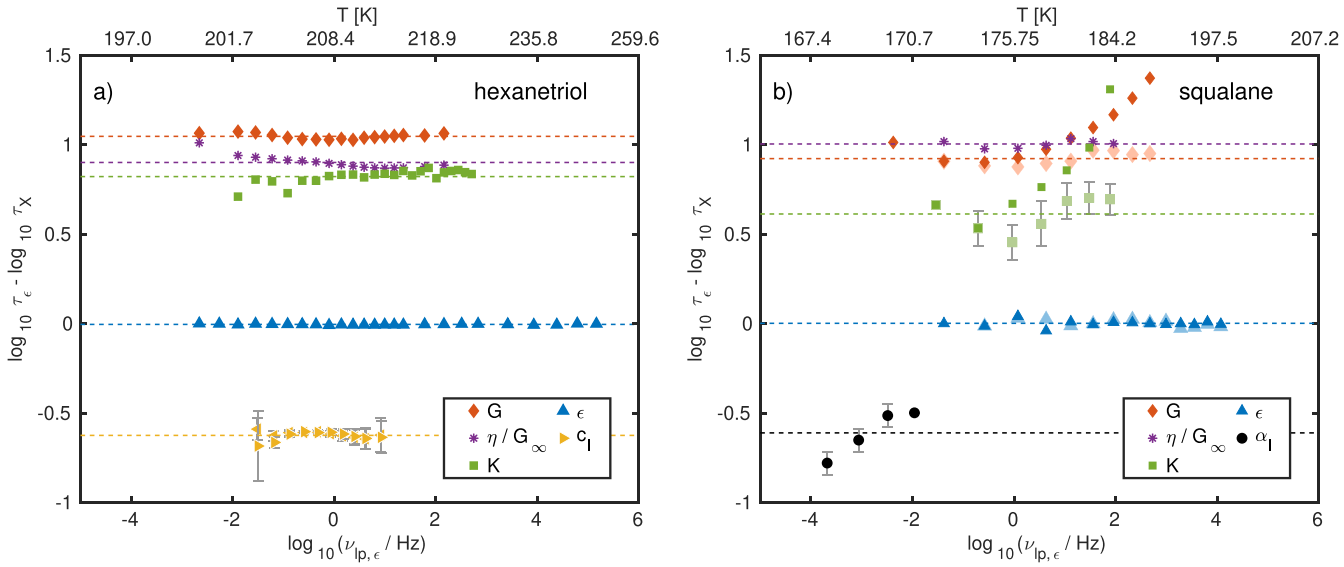

FIG. 8. Time-scale index for several response functions for hexanetriol in (a) and squalane in (b) based on the spectral loss-peak position (strong colors) and terminal modes (light colors) plotted as functions of the dielectric loss-peak frequency (bottom x-axis) and temperature (top x-axis). Dashed lines represent average values of the time-scale indices, based on the time scales derived from the loss-peak maximum for hexanetriol and the terminal mode for squalane with the exception of the expansivity data. Error bars were added in case the connected uncertainty exceeds the depicted symbols.

for hexanetriol resembles that of DC704 (see Fig. 9). For both materials, the time-scale indices are temperature-independent and the ordering of response-specific time scales is identical, suggesting that the intermolecular interactions of vdW- and hydrogen-bonded materials affect the coupling of time scales in a similar fashion. These findings are in accordance with the data reported for other alcohols.[12,16,22,23,34]

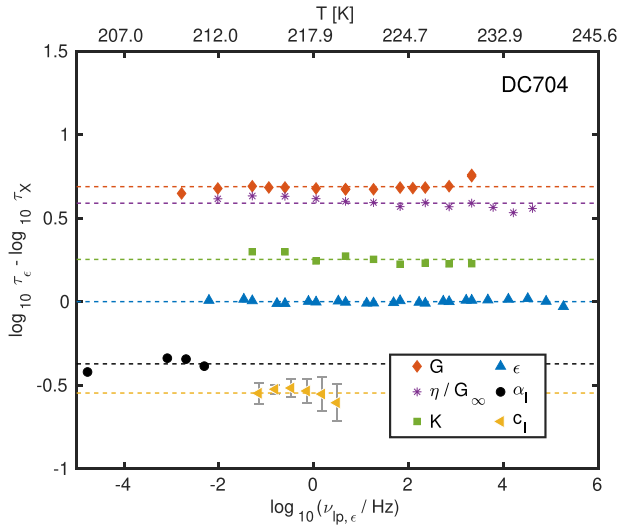

FIG. 9. Time-scale index for several response functions for DC704 plotted as functions of the dielectric loss-peak frequency (bottom x-axis) and temperature (top x-axis) from Ref. 8.

In contrast to the behavior observed for hexanetriol and DC704, time scales derived from loss-peak positions for squalane lead to temperature-dependent indices for the mechanical and dielectric response functions, as shown in Fig. 8(b). In previous studies, the apparent decoupling of time-scale indices for squalane was attributed to the influence of the secondary relaxation contribution on the position of the loss-peak maximum. Similar behavior was observed for other glass-forming liquids with a significant secondary relaxation contribution.[15,21,22] The index based on τ_M, however, related to the terminal relaxation mode, shows temperature-independent behavior. In analogy to τ_M, and in order to diminish the effect of the secondary contribution, time scales for dielectric, shear-mechanical, and bulk-mechanical data were extracted from their terminal mode [light-colored symbols in Fig. 8(b)]. The time scales based on the terminal mode lead to less temperature-dependent time-scale indices for all tested response functions. This strengthens the view that the secondary relaxation contribution is the origin of the time-scale decoupling reported in the literature for squalane. When considering the time-scale indices derived from the terminal mode, squalane clearly conforms to the same ordering of time scales as hexanetriol and DC704.

IV. SUMMARY

This study presents time-scale data based on five different response functions with a focus on the coupling tendency and the ordering of time scales. It is based on two liquids, hexanetriol and squalane, representing hydrogen-bonded liquids with a minor secondary relaxation contribution and vdW-binded liquids with a prominent secondary relaxation process. These data are set into context to results on the simple vdW-bonded liquids from Ref. 8.

The two major findings of the present study are (1) the general observation of time-scale coupling if the structural relaxation process dominates the response behavior and (2) identical ordering of response-function-specific time-scale indices. These observations are made for all the aforementioned liquids despite their fundamentally different inter-molecular interactions (vdW-bonded or hydrogen-bonded liquids) and the varying degrees of contributing relaxation processes (non-detectable, minor, strong secondary relaxation, or slow process) that occur in addition to the primary relaxation process.

In more detail, the poly-alcohol hexanetriol exhibits coupling of the time scales of structural relaxation over the full investigated temperature range based on the data from four response functions. This is in accordance with the observations on other poly-alcohols with minor secondary contribution, and it strengthens the view that the type of inter-molecular bonding has negligible effects on the coupling tendency for the investigated liquids. Continuing the discussion of the coupling behavior, squalane seems to oppose the observation made on hexanetriol on the first glance, as it shows clear signs of decoupling for time scales determined from spectral loss peak positions. This observation has also been observed for other materials with a dominant secondary relaxation contribution.[15,21] However, this behavior can be attributed to the influence of the secondary relaxation contribution rather than the dynamics of structural relaxation itself. This is confirmed by time-scale indices determined from the dynamics of the terminal mode, which is much less affected by the secondary relaxation contribution and result in approximately temperature-independent, i.e., constant time-scale indices.

Moreover, hexanetriol and squalane display the same order of response-function-specific time-scale indices as the simple vdW-bonded liquids from Ref. 8, indicating generic behavior for vdW- and hydrogen-bonded liquids,

$$\tau_G < \tau_K < \tau_\varepsilon < \tau_{\alpha_l} < \tau_{c_l}.$$

This finding, together with the observed time-scale coupling, indicates that the time scale ordering may be a more general feature of viscous liquids, extending beyond the simple liquids. It is especially surprising given that, for the more complex liquids studied here, the spectral shapes of the different response functions are vastly different. For the simple liquids studied in Ref. 8, the spectral shapes were nearly identical, and it was conjectured that these features are connected to the concept of simplicity.[25] As time-scale coupling and ordering hold for more complex vdW- and hydrogen-bonded liquids as well, it is reasonable to assume that the key characteristics of structural relaxation are of similar nature in all these types of liquids and are explicitly not dominated by the type of inter-molecular bonding. However, in complex materials, the structural relaxation is often obscured by additional relaxation processes, which lead to more complicated spectral shapes and differences in spectra obtained from different response functions. In agreement with this assumption, a comparison of spectral data based on light-scattering and dielectric spectroscopy for glycerol shows that self- and cross-correlated responses can be disentangled and strongly suggest comparable spectral shapes for the primary relaxation contributions measured by the two different response functions.[24] This view is further supported by the fact that, in many cases, the relaxation spectra can be fitted by assuming several spectral contributions, while shape parameters of the function describing the alpha relaxation are kept fixed.[23,38]

SUPPLEMENTARY MATERIAL

See the supplementary material for descriptions of experimental methods, time-domain expansivity data, normalized spectral data, details on electric-equivalent circuit models, and spectral data fitted to electric-equivalent circuit models.

ACKNOWLEDGMENTS

This work was funded by the VILLUM Foundation's Matter Grant (No. 16515).

DATA AVAILABILITY

The data that support the findings of this study are available at http://glass.ruc.dk/data/.

REFERENCES

[1] C. Angell, "Strong and fragile liquids," in *Relaxations in Complex Systems*, edited by K. L. Ngai and G. B. Wright (U.S. GPO, Washington, DC, 1985), pp. 3–11.
[2] J. C. Dyre, "The glass transition and elastic models of glass-forming liquids," Rev. Mod. Phys. **78**, 953–972 (2006).
[3] Y. S. Elmatad, D. Chandler, and J. P. Garrahan, "Corresponding states of structural glass formers," J. Phys. Chem. B **113**(16), 5563–5567 (2009).
[4] F. Pabst, J. Gabriel, P. Weigl, and T. Blochowicz, "Molecular dynamics of supercooled ionic liquids studied by light scattering and dielectric spectroscopy," Chem. Phys. **494**, 103–110 (2017).
[5] E. Shoifet, G. Schulz, and C. Schick, "Temperature modulated differential scanning calorimetry—Extension to high and low frequencies," Thermochim. Acta **603**, 227–236 (2015), part of Special Issue on Chip Calorimetry.
[6] L. A. Roed, T. Hecksher, J. C. Dyre, and K. Niss, "Generalized single-parameter aging tests and their application to glycerol," J. Chem. Phys. **150**(4), 044501 (2019).
[7] G. Harrison, *The Dynamic Properties of Supercooled Liquids* (Academic, London, 1976).
[8] B. Jakobsen, T. Hecksher, T. Christensen, N. B. Olsen, J. C. Dyre, and K. Niss, "Communication: Identical temperature dependence of the time scales of several linear-response functions of two glass-forming liquids," J. Chem. Phys. **136**, 081102 (2012).
[9] F. Stickel, E. W. Fischer, and R. Richert, "Dynamics of glass-forming liquids. II. Detailed comparison of dielectric relaxation, dc-conductivity, and viscosity data," J. Chem. Phys. **104**(5), 2043–2055 (1996).
[10] C. Hansen, F. Stickel, T. Berger, R. Richert, and E. W. Fischer, "Dynamics of glass-forming liquids. III. Comparing the dielectric α- and β-relaxation of 1-propanol and *o*-terphenyl," J. Chem. Phys. **107**(4), 1086–1093 (1997).
[11] R. Richert, K. Duvvuri, and L.-T. Duong, "Dynamics of glass-forming liquids. VII. Dielectric relaxation of supercooled *tris*-naphthylbenzene, squalane, and decahydroisoquinoline," J. Chem. Phys. **118**(4), 1828–1836 (2003).
[12] *The Scaling of Relaxation Processes*, edited by F. Kremer and A. Loidl (Springer, 2018).
[13] T. Christensen and N. B. Olsen, "Comparative measurements of the electrical and shear mechanical response functions in some supercooled liquids," J. Non-Cryst. Solids **172-174**, 357–361 (1994).
[14] M. Cutroni and A. Mandanici, "The α-relaxation process in simple glass forming liquid *m*-toluidine. II. The temperature dependence of the mechanical response," J. Chem. Phys. **114**(16), 7124–7129 (2001).
[15] B. Jakobsen, K. Niss, and N. B. Olsen, "Dielectric and shear mechanical alpha and beta relaxations in seven glass-forming liquids," J. Chem. Phys. **123**, 234511 (2005).

[16]T. Christensen and N. B. Olsen, "Quasistatic measurement of the frequency-dependent bulk and shear modulus of supercooled liquids," J. Non-Cryst. Solids **172-174**, 362–364 (1994).
[17]T. Hecksher, N. B. Olsen, K. A. Nelson, J. C. Dyre, and T. Christensen, "Mechanical spectra of glass-forming liquids. I. Low-frequency bulk and shear moduli of DC704 and 5-PPE measured by piezoceramic transducers," J. Chem. Phys. **138**(12), 12A543 (2013).
[18]D. Gundermann, K. Niss, T. Christensen, J. C. Dyre, and T. Hecksher, "The dynamic bulk modulus of three glass-forming liquids," J. Chem. Phys. **140**, 244508 (2014).
[19]L. A. Roed, K. Niss, and B. Jakobsen, "Communication: High pressure specific heat spectroscopy reveals simple relaxation behavior of glass forming molecular liquid," J. Chem. Phys. **143**(22), 221101 (2015).
[20]R. Casalini, S. S. Bair, and C. M. Roland, "Density scaling and decoupling in *o*-terphenyl, salol, and dibutyphthalate," J. Chem. Phys. **145**(6), 064502 (2016).
[21]R. Zorn, F. I. Mopsik, G. B. McKenna, L. Willner, and D. Richter, "Dynamics of polybutadienes with different microstructures. 2. Dielectric response and comparisons with rheological behavior," J. Chem. Phys. **107**(9), 3645–3655 (1997).
[22]B. Jakobsen, C. Maggi, T. Christensen, and J. C. Dyre, "Investigation of the shear-mechanical and dielectric relaxation processes in two monoalcohols close to the glass transition," J. Chem. Phys. **129**, 184502 (2008).
[23]M. H. Jensen, C. Gainaru, C. Alba-Simionesco, T. Hecksher, and K. Niss, "Slow rheological mode in glycerol and glycerol–water mixtures," Phys. Chem. Chem. Phys. **20**, 1716–1723 (2018).
[24]J. P. Gabriel, P. Zourchang, F. Pabst, A. Helbling, P. Weigl, T. Böhmer, and T. Blochowicz, "Intermolecular cross-correlations in the dielectric response of glycerol," Phys. Chem. Chem. Phys. **22**(20), 11644–11651 (2020).
[25]K. Niss and T. Hecksher, "Perspective: Searching for simplicity rather than universality in glass-forming liquids," J. Chem. Phys. **149**(23), 230901 (2018).
[26]B. Igarashi, T. Christensen, E. H. Larsen, N. B. Olsen, I. H. Pedersen, T. Rasmussen, and J. C. Dyre, "A cryostat and temperature control system optimized for measuring relaxations of glass-forming liquids," Rev. Sci. Instrum. **79**, 045105 (2008).
[27]B. Igarashi, T. Christensen, E. H. Larsen, N. B. Olsen, I. H. Pedersen, T. Rasmussen, and J. C. Dyre, "An impedance-measurement setup optimized for measuring relaxations of glass-forming liquids," Rev. Sci. Instrum. **79**(4), 045106 (2008).
[28]T. Christensen and N. B. Olsen, "A rheometer for the measurement of a high shear modulus covering more than seven decades of frequency below 50 kHz," Rev. Sci. Instrum. **66**, 5019 (1995).
[29]T. Christensen and N. B. Olsen, "Determination of the frequency-dependent bulk modulus of glycerol using a piezoelectric spherical shell," Phys. Rev. B **49**, 15396 (1994).
[30]K. Niss, D. Gundermann, T. Christensen, and J. C. Dyre, "Dynamic thermal expansivity of liquids near the glass transition," Phys. Rev. E **85**, 041501 (2012).
[31]T. Christensen, N. B. Olsen, and J. C. Dyre, "Can the frequency-dependent *isobaric* specific heat be measured by thermal effusion methods?," AIP Conf. Proc. **982**, 139 (2008), paper presented at the Fifth International Workshop on Complex Systems in Sendai 2007.
[32]B. Jakobsen, N. B. Olsen, and T. Christensen, "Frequency-dependent specific heat from thermal effusion in spherical geometry," Phys. Rev. E **81**, 061505 (2010).
[33]J. J. Papini, J. C. Dyre, and T. Christensen, "'cooling by heating'—Demonstrating the significance of the longitudinal specific heat," Phys. Rev. X **2**(4), 041015 (2012).
[34]M. Nakanishi and R. Nozaki, "Dynamics and structure of hydrogen-bonding glass formers: Comparison between hexanetriol and sugar alcohols based on dielectric relaxation," Phys. Rev. E **81**, 041501 (2010).
[35]T. Hecksher, N. B. Olsen, and J. C. Dyre, "Model for the alpha and beta shear-mechanical properties of supercooled liquids and its comparison to squalane data," J. Chem. Phys. **146**(15), 154504 (2017).
[36]K. Niss, J. C. Dyre, and T. Hecksher, "Long-time structural relaxation of glass-forming liquids: Simple or stretched exponential?," J. Chem. Phys. **152**(4), 041103 (2020).
[37]Y. S. Elmatad, D. Chandler, and J. P. Garrahan, "Corresponding states of structural glass formers. II," J. Phys. Chem. B **114**(51), 17113–17119 (2010).
[38]T. Blochowicz, C. Gainaru, P. Medick, C. Tschirwitz, and E. A. Rössler, "The dynamic susceptibility in glass forming molecular liquids: The search for universal relaxation patterns II," J. Chem. Phys. **124**(13), 134503 (2006).